

TENSILE CRACK TIP FIELDS IN ELASTIC-IDEALLY PLASTIC CRYSTALS

James R. RICE

Division of Applied Sciences, Harvard University, Cambridge, MA 02138, U.S.A.

Received 10 July 1987; revised version received 12 August 1987

Crack tip stress and deformation fields are analyzed for tensile-loaded ideally plastic crystals. The specific cases of (0 1 0) cracks growing in the [1 0 1] direction, and (1 0 1) cracks in the [0, 1, 0] direction, are considered for both fcc and bcc crystals which flow according to the critical resolved shear stress criterion. Stationary and quasistatically growing crack fields are considered. The analysis is asymptotic in character; complete elastic-plastic solutions have not been determined. The near-tip stress state is shown to be locally constant within angular sectors that are stressed to yield levels at a stationary crack tip, and to change discontinuously from sector to sector. Near tip deformations are not uniquely determined but fields involving shear displacement discontinuities at sector boundaries are required by the derived stress state. For the growing crack both stress and displacement must be fully continuous near the tip. An asymptotic solution is given that involves angular sectors at the tip that elastically unload from, and then reload to, a plastic state. The associated near-tip velocity field then has discontinuities of slip type at borders of the elastic sectors. The rays, emanating from the crack tip, on which discontinuities occur in the two types of solutions are found to lie either parallel or perpendicular to the family of slip plane traces that are stressed to yield levels by the local stresses. In the latter case the mode of concentrated shear along a ray of discontinuity is of kink type. Some consequences of this are discussed in terms of the dislocation generation and motion necessary to allow the flow predicted macroscopically.

Introduction

An asymptotic analysis of the crack tip stress and deformation field is presented for plane-strain tensile cracks in elastic-ideally plastic single crystals. Such crystals are assumed to have a limited set of possible slip systems and to have a critical resolved shear stress for plastic flow to occur on each. Here attention is limited to two specific crack orientations in face centered and body centered cubic crystals, although the analysis techniques are applicable to other orientations too.

One orientation considered is such that the crack plane is (0 1 0), i.e., parallel to a face of the reference cubic cell, and the crack tip lies along the face diagonal direction [1 0 $\bar{1}$]; the crack grows along the perpendicular face diagonal, [1 0 1]. See Fig. 1 for the fcc case and Fig. 2 for bcc. The analysis in all but the second to last section of the paper is discussed relative to that orientation. It

also happens to provide the solution for a second orientation considered, which still has the crack tip along the [1 0 $\bar{1}$] face diagonal but which has the crack plane as the (1 0 1) plane so that [0 1 0] is the direction of crack growth. Thus the second orientation has the crack line rotated 90° anticlockwise from what is pictured in Figs. 1(b) and 2(b). These two crack orientations are often, but not universally, encountered in experimental studies of cracking, whether by rapid cleavage, fatigue or chemically assisted crack growth, in ductile fcc and bcc metals (Tetelman and Robertson, 1963; Tetelman and Johnston, 1965; Neumann, 1974a, b; Garrett and Knott, 1975; Hecker et al., 1978; Rieux et al., 1979; Neumann et al., 1979; Vehoff and Neumann, 1979, 1980; Lynch, 1983, 1985; Sieradzki et al., 1984; Sieradzki and Newman, 1985; Pugh, 1985; Wang, 1987).

Figures 1 and 2 also show the slip systems which are assumed to be active in relaxing the crack tip stress concentration.

Yielding of an fcc crystal

In the fcc case one type of relaxing system involves either the $(1\ 1\ 1)$ or $(\bar{1}\ \bar{1}\ \bar{1})$ slip plane, i.e., the two traced by solid lines in Fig. 1(a). The fcc slip directions are along face diagonals of the reference cube and, consistently with the plane strain deformation mode considered, it is assumed that shear parallel to each slip plane involves simultaneous and equal amounts of slip along two face diagonal directions in that plane. For example, this means equal slip along the $[1\ \bar{1}\ 0]$ and $[0\ \bar{1}\ 1]$ directions on the $(1\ 1\ 1)$ slip plane in Fig. 1(a), so that the effective, composite, slip direction is $[1\ \bar{2}\ 1]$. Figure 1(b) shows the crack in the x_1, x_2 plane of deformation; traces of the slip planes just discussed are also shown as solid lines. Cartesian coordinates are attached here, and also in Fig. 2, such that x_1, x_2, x_3 are along the $[1\ 0\ 1], [0\ 1\ 0], [\bar{1}\ 0\ 1]$ directions, respectively.

Another combination of slip systems consistent with plane strain deformation involves simultaneous and equal shear on the pair of planes $(1\ 1\ \bar{1})$ and $(\bar{1}\ 1\ 1)$ (the latter of which is traced by dashed lines in Fig. 1(a)), with both slipping in the $[1\ 0\ 1]$ direction along which they intersect. Traces of these slip planes, where they intersect $x_3 = \text{constant}$, are shown by dashed lines in Fig. 1(b).

The particular combinations of slip systems identified are the only ones that can accommodate large plastic straining, as expected at a crack tip, under plane strain conditions, e.g., they are the only combinations that could be active in a rigid-plastic crystal under those conditions. Plastic straining on other slip systems or other combinations of systems produces a proportional plastic strain component ϵ_{33}^p . The total strain $\epsilon_{33} = \epsilon_{33}^e + \epsilon_{33}^p$ (elastic plus plastic) is bounded at a three-dimensional crack tip, and is assumed to be zero in the plane strain model. Also, the elastic strain ϵ_{33}^e stays bounded since the stresses are bounded near the crack tip (ideal plasticity). Thus it is clear that

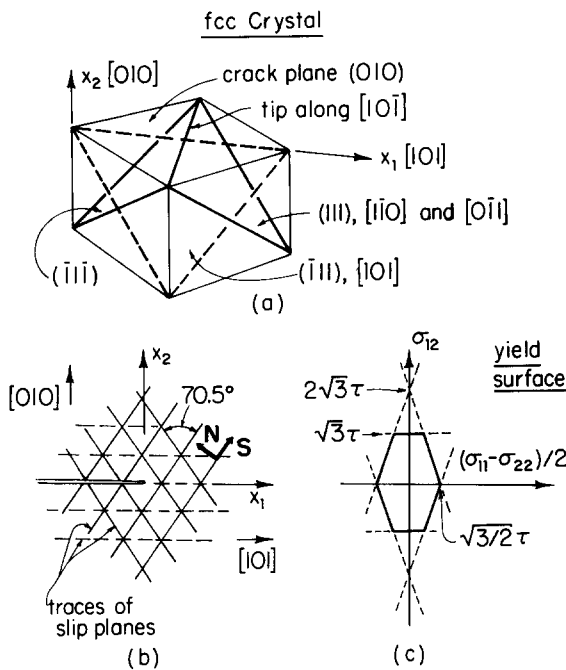


Fig. 1. (a) An fcc crystal with crack on (010) plane and tip along $[1\ 0\ \bar{1}]$ direction. Some slip systems capable of producing large plane strain plastic flow are indicated. (b) Crack in plane of deformation. Families of straight lines are traces of slip plane intersection with $x_3 = \text{constant}$; N and S are shown for one family. (c) Yield locus, where τ is the critical resolved shear stress on $\{111\}\langle 1\ \bar{1}\ 0\rangle$.

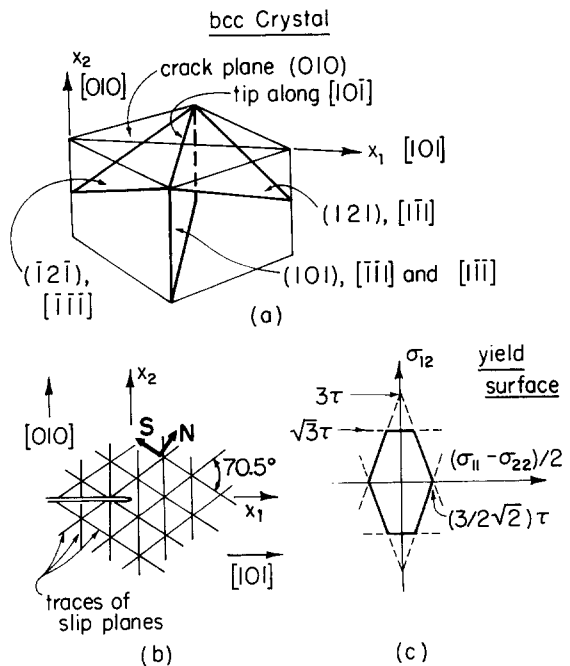


Fig. 2. Same as Fig. 1, but here for a bcc crystal. Yield locus shown for same critical stress τ on $\{121\}\langle 1\ \bar{1}\ 1\rangle$ and $\{101\}\langle 1\ \bar{1}\ \bar{1}\rangle$.

the other ignored slip systems or combinations could not contribute to a crack tip strain singularity. One cannot rule out the possibility that some secondary plastic strain does nevertheless occur on those systems, but they are ignored entirely here, as seems appropriate for a first analysis.

Yield surface as polygonal locus in σ_{12} and $\frac{1}{2}(\sigma_{11} - \sigma_{22})$ plane

Letting \mathbf{n} be the unit normal to a slip plane and \mathbf{s} a unit vector in the slip direction, the critical shear strength τ of that system is attained when $n_i \sigma_{ij} s_j = \pm \tau$. Here σ_{ij} is the stress and summation convention applies with Latin indices ranging over 1, 2, 3, but Greek indices over 1, 2 only. The yield surface in stress space, based on the particular slip system combinations compatible with large plane flow, is shown in Fig. 1(c). Rice (1973) explains why, for rigid-plastic incompressible solids with an associated flow rule (the case for crystals), the yield surface for plane strain is represented as a curve in a plane with axes $\frac{1}{2}(\sigma_{11} - \sigma_{22})$ and σ_{12} .

Each flat segment on the yield surface of Fig. 1(c) corresponds to plane strain shear relative to one of the three families of lines in Fig. 1(b), representing intersections of slip planes with $x_3 = \text{constant}$. It is convenient to describe yielding in terms of the geometry of those lines. Thus let $\mathbf{N} [= (N_1, N_2, 0)]$ be the unit vector normal to, and $\mathbf{S} [= (S_1, S_2, 0)]$ be a unit vector along, one of those line families. The vectors are shown for one of the inclined families in Fig. 1(b). Then the yield condition associated with that family can be written as $N_\alpha \sigma_{\alpha\lambda} S_\lambda = \pm \beta \tau$ (where $\beta = 2/\sqrt{3}$ for the inclined solid line families, and $\beta = \sqrt{3}$ for the crack-parallel dashed line family). Since $N_\alpha S_\alpha = 0$ and $S_1 = N_2, S_2 = -N_1$, this may be written also as

$$2N_1 N_2 \frac{(\sigma_{11} - \sigma_{22})}{2} + (N_2^2 - N_1^2) \sigma_{12} = \pm \beta \tau, \quad (1)$$

as a description of the corresponding line segment on the yield surface in stress space.

Strain hardening is neglected so that the yield locus is invariant to plastic deformation. Also, since the present study is formulated within the conventional small displacement gradient approximations of stress analysis, the apparent or

‘geometric’ hardening (or softening) which results when crystal slip systems rotate relative to material axes is neglected too. Both are important for inclusion in future work.

The bcc case

See Fig. 2. The slip direction in bcc is of $\langle 111 \rangle$ type, i.e., along the cube diagonal, and any low index plane containing this direction may serve as the slip plane; the $\{101\}$ and $\{121\}$ type planes are most common and are the only ones considered here. The three which can accommodate large plane-strain deformation (and require the lowest stress, when the critical τ is the same for all systems) are indicated in Fig. 2(a). Traces of the slip planes are shown in Fig. 2(b). They consist of the (121) plane with $[1\bar{1}1]$ slip, $(\bar{1}2\bar{1})$ plane with $[\bar{1}\bar{1}\bar{1}]$ slip, and (101) plane with (for consistency with plane strain) simultaneous and equal $[\bar{1}\bar{1}\bar{1}]$ and $[1\bar{1}\bar{1}]$ slip, combining effectively to $[0\bar{1}0]$. The yield locus is shown in Fig. 2(c) on the basis of the critical resolved shear stress condition, recognized as being less accurate for bcc than for fcc (e.g., Vitek, 1974, 1985). The factor $\beta = 1$ for yield of either of the $\{121\}$ type planes, whereas $\beta = \sqrt{3}$ for yield on the vertical (101) planes.

When the critical τ 's for $\{101\}$ and $\{121\}$ planes are not the same, the yield surface is capped at $\sqrt{3} \tau_{101}$ along the σ_{12} axis, whereas the intersection along the $\frac{1}{2}(\sigma_{11} - \sigma_{22})$ axis in Fig. 2(c) is at $(3/2\sqrt{2})\tau_{121}$, at least so long as $\tau_{121} < (2/\sqrt{3})\tau_{101}$. If that inequality is violated the yield surface becomes identical to that of Fig. 1(c) with τ understood as τ_{101} .

Interchange of \mathbf{N} and \mathbf{S}

The families of slip plane traces in the fcc and bcc case are identically oriented relative to one another, except that the slip plane traces for the bcc families are rotated by 90° relative to the traces for the fcc families (compare Figs. 1(b) and 2(b)). Put another way, if $\mathbf{N} = \mathbf{X}$ and $\mathbf{S} = \mathbf{Y}$ describe a particular fcc family, then $\mathbf{N} = \mathbf{Y}$ and $\mathbf{S} = \mathbf{X}$ describe a corresponding bcc family. The yield surface is invariant to interchange of \mathbf{N} and \mathbf{S} since they enter symmetrically into the yield condition $N_\alpha \sigma_{\alpha\lambda} S_\lambda = \beta \tau$. Thus the flat segments on

tions as those on the yield surface for bcc, as seen by comparing Figs. 1(c) and 2(c). The two cases differ only insofar as the β 's are different and the relative location of the cut-offs along the σ_{12} axis differ.

In fact, in the present 'small strain' (to use a common misnomer) formulation, which neglects effects of rotation of the lattice relative to the material, all the equations of the formulation are invariant under interchange of N and S on all the families of slip plane traces. The interchange corresponds to rotating all traces by 90° . Thus the solutions developed here for the fcc and bcc cases will be essentially identical, apart from the minor effects of the different β 's (which merely scale the near tip stresses when expressed as $\sigma_{\alpha\lambda}/\beta\tau$) and the different relative positions of the cut-offs along the σ_{12} axis. Only the spin of the lattice relative to the material, neglected in the present formulation but which reverses sign under interchange of N and S , causes a change when we compare solutions for two such families of slip plane traces which differ from one another by a 90° rotation. Related discussion is given by Rice and Nikolic (1985) for the anti-plane case, and in the closing discussion here.

Equilibrium stress distributions

Let r, θ be polar coordinates centered at the crack tip such that

$$x_1 = a + r \cos \theta, \quad x_2 = r \sin \theta, \quad (2)$$

where a is crack length as measured from the (fixed) x_1, x_2 coordinate origin ($a=0$ in Figs. 1(b), 2(b)). The tip will, in different circumstances, be regarded as being stationary while the cracked crystal is being loaded, or as moving ($\dot{a} > 0$) quasistatically through the loaded crystal.

Following methods of asymptotic crack tip analysis of ideally plastic materials as summarized by Rice (1982), in the presence of a bounded crack tip stress state the equilibrium equations

$$\frac{\partial \sigma_{\alpha\beta}}{\partial x_\alpha} = \left(\frac{\partial \sigma_{\alpha\beta}}{\partial r} \right) e_\alpha + \left(\frac{\partial \sigma_{\alpha\beta}}{\partial \theta} \right) \frac{e'_\alpha}{r} = 0 \quad (3)$$

require that

$$e'_\alpha \sigma'_{\alpha\beta} = 0. \quad (4)$$

Here $e_\alpha = \partial r / \partial x_\alpha = e_\alpha(\theta)$, with $(e_1, e_2) = (\cos \theta, \sin \theta)$, is the radial unit vector in the x_1, x_2 plane, $e'_\alpha \equiv de_\alpha/d\theta$ is a unit vector in the direction of increasing θ (hence $e'_\alpha e_\alpha = 0$ and $e'_\alpha = r \partial \theta / \partial x_\alpha$), and $\sigma'_{ij} = \sigma'_{ij}(\theta)$ denotes

$$\sigma'_{ij} = \lim_{r \rightarrow 0} \left[\partial \sigma_{ij}(r, \theta) / \partial \theta \right]. \quad (5)$$

Since $\sigma'_{\alpha\beta}$ is symmetric we must likewise have $\sigma'_{\alpha\beta} e'_\beta = 0$, and since $e_\gamma e'_\gamma = 0$, such implies that $\sigma'_{\alpha\beta}$ has the form $\lambda e_\alpha e_\beta$. After a little calculation one then confirms that all bounded near tip stress states consistent with equilibrium must satisfy

$$\sigma'_{\alpha\beta} = e_\alpha e_\beta (\sigma'_{11} + \sigma'_{22}). \quad (6)$$

Now suppose that a particular angular sector at the crack tip is at yield, i.e., its stress state lies on the yield locus. If that state involves the critical condition $N_\alpha \sigma_{\alpha\lambda} S_\lambda = \beta\tau$, then $N_\alpha \sigma'_{\alpha\lambda} S_\lambda = 0$ within the sector. By (6), this requires that

$$(N_\alpha e_\alpha)(S_\lambda e_\lambda)(\sigma'_{11} + \sigma'_{22}) = 0. \quad (7)$$

Thus, for all θ except the four special values for which e has the same line of action as either N or S , this condition requires that $\sigma'_{11} + \sigma'_{22} = 0$. By (6), this implies that all $\sigma'_{\alpha\lambda} = 0$, and thus stress states (as $r \rightarrow 0$) in angular sectors which are at yield must be of the 'constant stress' type, $\sigma_{\alpha\lambda} = \text{constant}$ (i.e., independent of θ) for all α, λ except possibly at the four special values of θ .

Clearly, for a tensile-loaded crack with $\sigma_{22} \neq 0$ on $\theta = 0$, a stress distribution involving constant $\sigma_{\alpha\lambda}$ at all θ cannot meet crack surface boundary conditions. Thus it is necessary that either (i) the stresses in some angular sector at the tip not be at yield, or (ii) that the stresses change discontinuously at certain angles θ (possibly one of those noted above, for which the line of action of e aligns with N or S).

Option (ii) is not possible for the quasistatically growing crack, since Drugan and Rice (1984) have shown that an arc across which $\sigma_{\alpha\lambda}$ is discontinuous cannot move normal to itself in the type of elastic-plastic solid considered here. Thus, for the quasistatically growing crack it will be necessary

that option (i) be followed, and the solution to be presented for that case does indeed involve angular sectors in which elastic unloading (and reloading) occurs. Option (ii), i.e., discontinuity of stress, cannot be ruled out for the stationary crack, and we analyze that case next.

Discontinuities of stress and stationary crack tip fields

We attempt to find a solution, appropriate for a stationary tensile crack, that is consistent with active plastic flow occurring at all angles about the crack tip. As just noted, this will be possible only if the near tip stress state is discontinuous.

Suppose, then, that on a ray of direction e , $[[\sigma_{\alpha\lambda}]]$ is nonzero. Here $[[f]] = f(\theta^+) - f(\theta^-)$. Continuity of the traction vector requires that

$$e'_\alpha [[\sigma_{\alpha\lambda}]] = 0 \tag{8}$$

on that ray, and since $\sigma_{\alpha\lambda} = \sigma_{\lambda\alpha}$, this requires, by reasoning similar to that in going from (4) to (6), that any such discontinuity must satisfy

$$[[\sigma_{\alpha\lambda}]] = e_\alpha e_\lambda [[\sigma_{11} + \sigma_{22}]]. \tag{9}$$

Now, if the yield condition is to be met at all angles about the tip, the discontinuity must carry the stress state from one point to another of a yield locus like in Fig. 1(c) or 2(c). By (9), the locus of stress states encountered on traversing that discontinuity must lie along a straight line in the stress space joining those two points (thinking of the discontinuity as the limit of thin zone of rapid transition).

However, if we seek a solution corresponding to yield at all angles about the tip, and extend this requirement to all states traversed in crossing the discontinuity, then we must require that the line joining those two points on the yield locus also lies along the yield locus. Hence the two points considered must lie on the same straight line segment of the yield locus. (Otherwise, the stress states traversed at the discontinuity would correspond to elastic unloading).

If N , S correspond to that straight line segment, then $N_\alpha S_\lambda \sigma_{\alpha\lambda}$ is the same on both sides of

the discontinuity, so that

$$0 = N_\alpha S_\lambda [[\sigma_{\alpha\lambda}]] = (N_\alpha e_\alpha)(S_\lambda e_\lambda) [[\sigma_{11} + \sigma_{22}]]. \tag{10}$$

Thus, as already anticipated, a discontinuity is possible when e has the same line of action as either N or S .

Thus, with reference to the families of slip plane traces in Figs. 1(b) and 2(b), a stress field corresponding to plastic activity on a particular family may have a discontinuity along either the member of that family passing through the crack tip, or along the line through the tip that is perpendicular to that member. As experience in constructing discontinuous stress states consistent with these requirements shows, the stress state must change from vertex to vertex of the yield locus at a discontinuity. If the end state does not reach a vertex, the possibility for a further discontinuous jump will not occur until 90° change in θ and, in the cases examined, such situations do not allow construction of a solution.

Stress field at stationary crack tip

Figure 3 illustrates the solutions constructed in this manner. The situation for both fcc and bcc are shown on the same diagram since the positions of the resulting rays of discontinuity turn out to be the same for both.

Figure 3 (and the labelling of yield surfaces for the two cases in Figs. 1(c) and 2(c)) provides the distribution of σ_{12} and $\frac{1}{2}(\sigma_{11} - \sigma_{22})$. To obtain $\sigma_{11} + \sigma_{22}$, observe that at each discontinuity surface

$$\begin{aligned} [[\sigma_{12}]] &= e_1 e_2 [[\sigma_{11} + \sigma_{22}]], \\ [[\sigma_{11} - \sigma_{22}]] &= (e_1^2 - e_2^2) [[\sigma_{11} + \sigma_{22}]], \end{aligned} \tag{11}$$

where e is the direction of the ray along which the discontinuity occurs. Since

$$(e_1^2 - e_2^2)^2 + 4e_1^2 e_2^2 = 1,$$

this gives (with due regard to sign for the application here)

$$[[\frac{1}{2}(\sigma_{11} + \sigma_{22})]] = -[[L]] \tag{12}$$

at each discontinuity. Here L is the arc length around the yield surface, having units of stress and increasing in the direction $A \rightarrow B \rightarrow C \rightarrow D$,

Stationary Crack

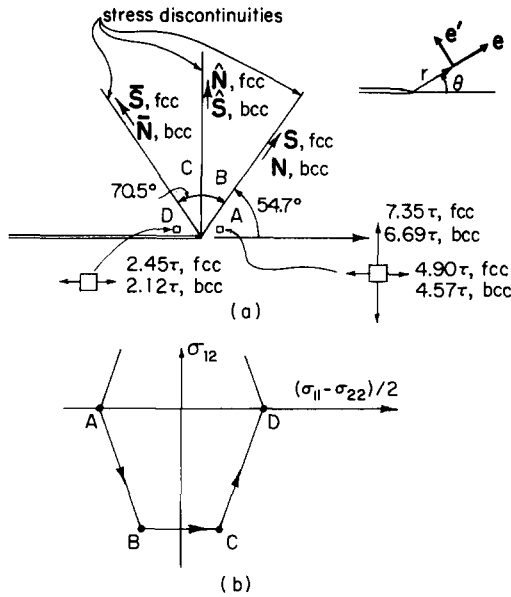


Fig. 3. (a) Stress state at a stationary crack tip is constant within angular sectors at a crack tip and jumps discontinuously at sector boundaries. Same discontinuity locations for fcc and bcc case. Inset: unit vector e in radial direction, e' in circumferential. (b) Points on yield locus corresponding to constant stress sectors above. See Table 1.

such that for each jump from one vertex to the next

$$[L]^2 = [\sigma_{12}]^2 + \left[\frac{1}{2}(\sigma_{11} - \sigma_{22})\right]^2. \quad (13)$$

Equation (12) can also be regarded as a consequence of equations which arise in the generalization of plane strain slip line theory to the anisotropic case (Booker and Davis, 1972; Rice, 1973), in which case $\frac{1}{2}(\sigma_{11} + \sigma_{22}) + L$ is constant along a line of one family of characteristics and $\frac{1}{2}(\sigma_{11} + \sigma_{22}) - L$ along a line of the other family.

Equation (12) is used in the following way. For sector D , the boundary condition requires $\sigma_{22}^D = 0$. Thus

$$\frac{1}{2}(\sigma_{11}^D + \sigma_{22}^D) = \frac{1}{2}(\sigma_{11}^D - \sigma_{22}^D), \quad (14)$$

where the latter can be read off from the yield loci in Figs. 1(c) and 2(c). (It is $(\sqrt{3}/\sqrt{2})\tau$ for the fcc case, and $(3/2\sqrt{2})\tau$ for the bcc case.) One there-

Table 1
Stress field at stationary crack tip

| Sector | σ_{22}/τ | σ_{11}/τ | σ_{12}/τ |
|--|----------------------------------|--------------------------------------|------------------------|
| <i>fcc stresses</i> [$\tau = \tau_{(111)\langle 10\bar{1}\rangle}$] | | | |
| A 0° – 54.74° | $3\sqrt{6}$ (7.35) | $2\sqrt{6}$ (4.90) | 0 |
| B 54.74° – 90° | $2\sqrt{6}$ (4.90) | $3\sqrt{6}/2$ (3.67) | $-\sqrt{3}$ (-1.73) |
| C 90° – 125.26° | $\sqrt{6}$ (2.45) | $3\sqrt{6}/2$ (3.67) | $-\sqrt{3}$ (-1.73) |
| D 125.26° – 180° | 0 | $\sqrt{6}$ (2.45) | 0 |
| <i>bcc stresses</i> [$\tau = \tau_{(121)\langle 1\bar{1}\bar{1}\rangle} = \tau_{(101)\langle 11\bar{1}\rangle}$] | | | |
| A 0° – 54.74° | $\sqrt{6} + 3\sqrt{2}$ (6.69) | $\sqrt{6} + 3\sqrt{2}/2$ (4.57) | 0 |
| B 54.74° – 90° | $3\sqrt{2}$ (4.24) | $\sqrt{6}/2 + 3\sqrt{2}/2$ (3.35) | $-\sqrt{3}$ (-1.73) |
| C 90° – 125.26° | $\sqrt{6}$ (2.45) | $\sqrt{6}/2 + 3\sqrt{2}/2$ (3.35) | $-\sqrt{3}$ (-1.73) |
| D 125.26° – 180° | 0 | $3\sqrt{2}/2$ (2.12) | 0 |

fore has

$$\begin{aligned} (\sigma_{11}^C + \sigma_{22}^C)/2 &= (\sigma_{11}^D - \sigma_{22}^D)/2 + L_{CD}, \\ (\sigma_{11}^B + \sigma_{22}^B)/2 &= (\sigma_{11}^C + \sigma_{22}^C)/2 + L_{BC}, \\ (\sigma_{11}^A + \sigma_{22}^A)/2 &= (\sigma_{11}^B + \sigma_{22}^B)/2 + L_{AB}, \end{aligned} \quad (15)$$

for successive calculation of $\sigma_{11} + \sigma_{22}$ in the different sectors. The full stress state is given in Table 1. For example, the maximum tension occurs in sector A and is $\sigma_{22}^A = 7.35\tau$ for the fcc and 6.69τ for the bcc case.

Plastic limit state fields

The fields constructed at the crack tip in Fig. 3 are identical, apart from the sign of stresses, to what Rice (1973) derived as the field at the corner of a flat-ended, frictionless, rigid punch which indents an anisotropic rigid-plastic half space under plane strain conditions. See also Pan (1986). These fields are the analogs, for single crystal plasticity, of the Prandtl slip line field, introduced

in connection with punch indentation (e.g., Hill, 1950) for isotropic materials, and which also arises in representing the plane strain state at a crack tip in such isotropic materials (Rice, 1967).

Other crack tip stress fields can also be devised, just as in the isotropic case. Those involve either angular sectors at the crack tip that are stressed below yield levels, or discontinuities for which stress states traversed at the discontinuity surface are below yield levels, or both. These fields produce less stress σ_{22} ahead of the crack than do those presented in Fig. 3 (as may be shown by considering the bounding theorems of limit analysis). However, such fields with lower stress may actually arise for fully plastic loading of some geometries, e.g., for the plane strain tension of a bar with an internal crack, in which case the triaxial stress elevation of the Prandtl-like fields cannot be maintained.

By analogy to the punch problem, the stress field at each crack tip for fully plastic (limit load) extension of a solid with deep double edge cracks, Fig. 4(a), is the same as given in Fig. 3 and Table 1. See Rice (1973) for the kinematics of the fully plastic flow field. However, the bounding theo-

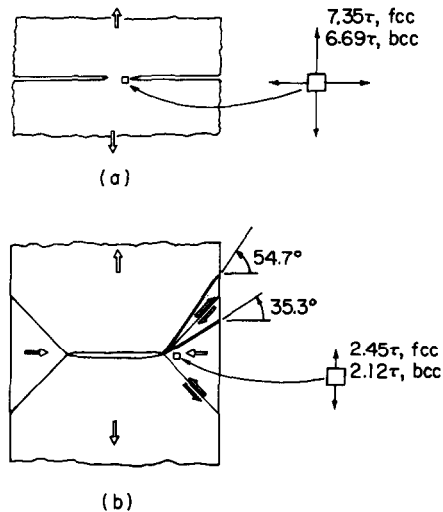


Fig. 4. Fully plastic crystals, deformed in tension at plastic limit load. (a) Very deep double edge cracks; crack tip stress state same as Fig. 3 and Table 1. (b) Internally cracked tensile geometry. Stress state with $\sigma_{11} = 0$ ahead of crack; flow field consistent with concentrated shear deformation along any ray within the range indicated.

rems of limit analysis may be applied to the internally cracked bar, Fig. 4(b), to show that at fully plastic conditions the stress state directly ahead of the crack is $\sigma_{12} = \sigma_{11} = 0$,

$$\sigma_{22} = \begin{cases} \sqrt{6} \tau = 2.45 \tau & \text{for the fcc case,} \\ (3/\sqrt{2}) \tau = 2.12 \tau & \text{for the bcc case.} \end{cases} \quad (16)$$

The limit state flow field for the internally cracked bar is nonunique but it can involve concentrated shear (i.e., a slip velocity discontinuity) along any ray or set of rays, including a continuous distribution of rays, from the crack tip within the limits set by the two rays indicated in Fig. 4(b). The limits themselves correspond to concentrated shear involving only one or the other of the two families of slip plane traces that are active at the vertex to which the stress state corresponds. The upper limiting ray shown is along the active slip plane traces (like in Fig. 5(a)) in the fcc case but perpendicular to the active traces (as in Fig. 5(b)) for the bcc case. The lower limiting ray is perpendicular to the active traces in the fcc case but along them in the bcc case. Experiments on fully plastic deformation of single edge notched crystal bars of Cu and Fe-3%Si by Neumann (1974a), Neumann et al. (1979) and Vehoff and

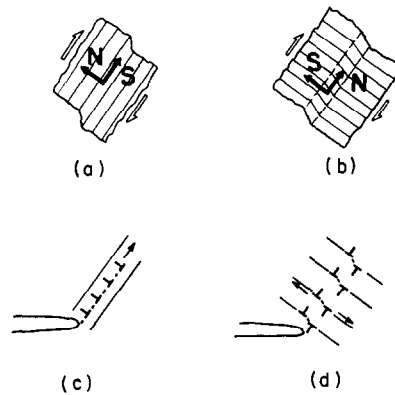


Fig. 5. (a) Regular and (b) kinking mode of concentrated shear; S is along slip plane trace and N is normal to it. (c) Shear like in (a) can be accomplished by sweeping dislocations generated at crack tip out along slip planes. (d) Kinking shear requires abundant internal dislocation sources, from which loops expand in a dipole mode to produce macroscopically concentrated shear (and lattice rotation).

Neumann (1979, 1980) evidently activate a mode of flow like that in Fig. 4(b).

Those experiments involve cyclic loading, and, at least in that situation, the observed deformation seems to occur primarily along a zone of concentrated shear that is essentially coincident with a slip plane trace emanating from the tip. For the fcc orientation of Fig. 1, that would correspond to the upper limiting ray in Fig. 4(b). Nevertheless, the experiments on Cu in that orientation also show evidence (Neumann et al., 1979, Figs. 6 and 7) of more limited activation of the second set of slip plane traces, stressed to yield by the vertex stress state ahead of the crack. Further, the observed boundaries of the plastically deforming zone ahead of the tip coincides with the two limiting angles of Fig. 4(b). That is, the lower boundary lies perpendicular to the (second) set of slip plane traces which, alone, are active in that part of the deforming region. Neumann et al. (1974) refer to that boundary as a 'tilt boundary'.

It is important to realize that, by comparison to the fully plastic geometry of Fig. 4(b), a more complex stress state with substantial triaxial stress elevation and activation of additional slip systems, as in Fig. 3, results for more constrained geometries like the fully plastic configuration of Fig. 4(a) and, presumably, for small scale yielding.

Strain distribution and displacement discontinuities

At the level of analysis attempted here, it is not possible to characterize in detail the near tip strain field associated with the stress state of Fig. 3. The stress state is everywhere at one or another vertex on the yield surface. Thus the stress state is always such that at each point two of the three families of slip line traces in Figs. 1(b) or 2(b) are simultaneously stressed to yield. If N and \hat{N} denote their normals, and S and \hat{S} the slip directions (so that shear strain of type γ_{NS} is positive when the system is active), the plastic strain rate tensor has the form

$$\begin{aligned} \dot{\epsilon}_{\alpha\lambda}^p = & \Lambda (N_\alpha S_\lambda + N_\lambda S_\alpha) \\ & + \hat{\Lambda} (\hat{N}_\alpha \hat{S}_\lambda + \hat{N}_\lambda \hat{S}_\alpha) \end{aligned} \quad (17)$$

where $\Lambda \geq 0$ and $\hat{\Lambda} \geq 0$.

At the rays along which stress discontinuities

occur, Fig. 3, the pair of slip plane traces which are stressed at yield changes from the pair with normals, say, \bar{N} , \bar{N} , to the pair with normals, say, \bar{N} , \hat{N} . As noted earlier, the ray on which such occurs is either in the direction of \hat{S} or \hat{N} (i.e., either along the slip line trace or perpendicular to it). For example, the inclined discontinuity rays in Fig. 3 lie along the plastically active $\{1\ 1\ 1\}$ plane traces in the fcc example, but they are perpendicular to traces of the plastically active $\{1\ 2\ 1\}$ slip planes in the bcc case. That is, they are in the direction of S for fcc and N for bcc. The situation reverses for the vertical discontinuity rays. They are perpendicular to the active $\{1\ 1\ 1\}$ slip plane traces for fcc, but along a trace of the active $\{1\ 0\ 1\}$ plane for bcc.

The family of deformation fields consistent with the crack tip stress state derived includes fields for which the displacement vector has discontinuities, of shear type, along the same rays across which the stress is discontinuous. These correspond to concentrated shear parallel to slip plane traces when the ray direction corresponds to S , and to kink-like shear perpendicular to those traces when the ray direction is N . See Fig. 5(a) for the former, 5(b) for the latter.

In fact, one may show as follows that shear displacement discontinuities must occur along the rays where the stress discontinuities occur. Observe that the stress discontinuities are such that $[[\sigma_{rr}]] < 0$ at each sector boundary, where $\sigma_{rr} = e_\alpha \sigma_{\alpha\beta} e_\beta$; other polar coordinate stress components are continuous. Thus, dividing strain $\epsilon_{\alpha\beta}$ into elastic and plastic parts, $\epsilon_{\alpha\beta}^e + \epsilon_{\alpha\beta}^p$, $[[\epsilon_{rr}^e]] < 0$. Also, examination of the actively stressed pairs of slip plane traces near each discontinuity shows in every case that $\epsilon_{rr}^p \geq 0$ on the $-$ side and $\epsilon_{rr}^p \leq 0$ on the $+$ side. Thus $[[\epsilon_{rr}^p]] \leq 0$, so that $[[\epsilon_{rr}]] < 0$, at the sector boundary. Since $\epsilon_{rr} = \partial u_r / \partial r$, where u_r is the radial displacement, one has a nonzero gradient of $[[u_r]]$ along the sector boundary. Thus, presuming that the stress discontinuity defining that boundary extends finitely from the crack tip, $[[u_r]] \neq 0$, i.e., there must be a shear displacement discontinuity at the sector boundary.

An analogous discussion could be given for antiplane shear of ductile crystals based on a similar asymptotic analysis (Rice and Nikolic,

1985). However, in the antiplane case the full elastic-plastic solution can be derived for the stationary crack in a crystal based on a method by Rice (1967, 1984). It turns out in the full solution that all plastic flow is confined to a set of rays across which the stress changes discontinuously, and these planar plastic zones, emanating from the tip, are surfaces of shear displacement discontinuity.

Quasistatically growing crack; elastic unloading and reloading sectors

As remarked earlier, equilibrium stress states which are at plastic yield for the crystals considered cannot vary with θ , except at special angles where discontinuities cannot be precluded. However, a fuller consideration of the relevant set of equations (Drugan and Rice, 1984), including the incremental stress-strain relations, shows that such discontinuities of stress are not allowed for the quasistatically growing crack. Thus option (i) of the earlier discussion must apply. Any plastic angular sectors, necessarily of constant stress type, must border sectors in which elastic unloading (and perhaps loading) occurs. [A fuller analysis in which one does not, as here, disregard the possible activation of slip systems that are incapable of sustaining large plane deformation may lead to sectors which are analogous to the ‘nonsingular’ plastic sectors of Rice (1982, Section 4.4) and Drugan et al. (1982). Those are sectors which are at yield but in which changes in plastic strain occur that remain bounded as $r \rightarrow 0$.]

Under plane strain conditions with elastic response, although of material that may have previously yielded, the constitutive relation is

$$\frac{\partial v_\alpha}{\partial x_\beta} + \frac{\partial v_\beta}{\partial x_\alpha} = 2c_{\alpha\beta\gamma\delta}\dot{\sigma}_{\gamma\delta} \tag{18}$$

where $c_{\alpha\beta\gamma\delta}$ is the two-dimensional compliance tensor. It is related to the corresponding three-dimensional compliance M_{ijkl} by

$$c_{\alpha\beta\gamma\delta} = M_{\alpha\beta\gamma\delta} - \frac{M_{\alpha\beta 33}M_{33\gamma\delta}}{M_{3333}} \tag{19}$$

assuming that the symmetry of the crystal makes

$\sigma_{13} = \sigma_{23} = 0$ as in the cases considered here. Since $\dot{\theta}$, the rate of change of θ at a fixed material point, is given by $e_2\dot{a}/r$ ($e_2 = \sin \theta$) the dominant, singular term in the near tip stress rate is

$$\dot{\sigma}_{\gamma\delta} = \sigma'_{\gamma\delta}\dot{\theta} = (e_2\dot{a}/r)\sigma'_{\gamma\delta}. \tag{20}$$

When the requirements of equilibrium (6) are enforced this becomes

$$\dot{\sigma}_{\gamma\delta} = (e_2\dot{a}/r)e_\gamma e_\delta(\sigma'_{11} + \sigma'_{22}). \tag{21}$$

Evidently, the velocity gradients must be singular as $1/r$ in such elastic sectors. An easy analysis reveals that the most general form of velocity field consistent with such a $1/r$ velocity gradient singularity is

$$v_\alpha = \dot{a} B_\alpha \ln(R/r) + \dot{a} g_\alpha(\theta) \tag{22}$$

where the B 's are constants and R is some constant length. When the velocity gradients are computed from (22) and the stress rate taken from (21), (18) requires that

$$\begin{aligned} -B_\alpha e_\beta - B_\beta e_\alpha + g'_\alpha e'_\beta + g'_\beta e'_\alpha \\ = 2e_2 c_{\alpha\beta\gamma\delta} e_\gamma e_\delta (\sigma'_{11} + \sigma'_{22}). \end{aligned} \tag{23}$$

The notations

$$\begin{aligned} c_{11} &= c_{11}(\theta) = e_\alpha e_\beta c_{\alpha\beta\gamma\delta} e_\gamma e_\delta, \\ c_{21} &= c_{21}(\theta) = e'_\alpha e'_\beta c_{\alpha\beta\gamma\delta} e_\gamma e_\delta, \\ c_{41} &= c_{41}(\theta) = 2e'_\alpha e'_\beta c_{\alpha\beta\gamma\delta} e_\gamma e_\delta, \end{aligned} \tag{24}$$

are introduced. Here the indices 1, 2 and 4 have nothing to do with the Cartesian directions but rather correspond to the standard subscript designations for crystal elastic compliances, denoted s'_{mn} , e.g., by Hirth and Lothe (1968, chp. 13), here relative to axes in the r , θ and x_3 directions. For an elastically isotropic solid, $c_{11} = (1 - \nu)/2\mu$, $c_{21} = -\nu/2\mu$ and $c_{41} = 0$; here μ = shear modulus and ν = Poisson ratio.

When (23) is multiplied by the pairs $e_\alpha e_\beta$, $e'_\alpha e'_\beta$, and $e'_\alpha e'_\beta$ there results the fully equivalent set of equations

$$-B_\alpha e_\alpha = e_2 c_{11}(\sigma'_{11} + \sigma'_{22}), \tag{25}$$

$$g'_\alpha e'_\alpha = e_2 c_{21}(\sigma'_{11} + \sigma'_{22}), \tag{26}$$

$$-B_\alpha e'_\alpha + g'_\alpha e_\alpha = e_2 c_{41}(\sigma'_{11} + \sigma'_{22}). \tag{27}$$

These may be solved for $\sigma'_{11} + \sigma'_{22}$ and for g'_α .

Thus the form of the limiting stress field as $r \rightarrow 0$ in angular sectors at the crack tip which respond elastically is, using the solution for $\sigma'_{11} + \sigma'_{22}$ in (25) and then integrating (6) on θ ,

$$\sigma_{\alpha\beta} = \sigma_{\alpha\beta}^0 - B_\lambda \int_{\theta^0}^{\theta} \left[\frac{e_\alpha(\bar{\theta}) e_\beta(\bar{\theta}) e_\lambda(\bar{\theta})}{e_2(\bar{\theta}) c_{11}(\bar{\theta})} \right] d\bar{\theta}. \quad (28)$$

Here the sector is presumed to begin at angle θ^0 where the stress is $\sigma_{\alpha\beta}^0$. Also, the near-tip velocity field is obtained by using the solution for $g'_\alpha(\theta)$ above and integrating, to obtain

$$v_\alpha = \dot{a} B_\alpha \ln(R/r) + \dot{a} B_\beta \int_{\theta^0}^{\theta} \left\{ e_\alpha(\bar{\theta}) e'_\beta(\bar{\theta}) - [e'_\alpha(\bar{\theta}) e_\beta(\bar{\theta}) c_{21}(\bar{\theta}) + e_\alpha(\bar{\theta}) e_\beta(\bar{\theta}) c_{41}(\bar{\theta})] / c_{11}(\bar{\theta}) \right\} d\bar{\theta} + \dot{a} G_\alpha^0. \quad (29)$$

Here the constants $G_\alpha^0 = g_\alpha(\theta^0)$ and, together with the constant R , correspond to purely translational motion. Thus the entire field of stress and velocity is represented in terms of the two constants B_1 and B_2 and conditions at a sector boundary. This analysis applies to an elastic sector of finite stress at a quasistatically moving crack tip in any material, and is equivalent to that given by Rice (1982, Section 4.3); B_α here is $-A_\alpha$ in his equations.

Conditions at plastic boundaries of elastic unloading and reloading sectors

Suppose that the elastic unloading sector lies in the range $\theta^0 < \theta < \theta^1$, where $\theta^0 > 0$, $\theta^1 < \pi$, and that the stress state is plastic at both limits of this range. If the stress is consistent with yield on a line family of slip plane traces with normal N^0 and (positive) slip direction S^0 at $\theta = \theta^0$, and with N^1 and S^1 at $\theta = \theta^1$, then the unloading and reloading conditions

$$N_\alpha^0 S_\beta^0 \dot{\sigma}_{\alpha\beta} \leq 0 \quad \text{at } \theta = \theta^{0+};$$

$$N_\alpha^1 S_\alpha^1 \dot{\sigma}_{\alpha\beta} \geq 0 \quad \text{at } \theta = \theta^{1-} \quad (30)$$

must be met. Using (21) for $\dot{\sigma}_{\alpha\beta}$ and (25), these become

$$N_\alpha^0 e_\alpha S_\beta^0 e_\beta B_\lambda e_\lambda \geq 0 \quad \text{at } \theta^{0+} \quad (31)$$

and

$$N_\alpha^1 e_\alpha S_\beta^1 e_\beta B_\lambda e_\lambda \leq 0 \quad \text{at } \theta^{1-} \quad (32)$$

Further, if the state at either θ^0 or θ^1 or both is of vertex character, simultaneously yielding two families of planes, then the corresponding inequality must apply for the pair of vectors N , S and \bar{N} , \bar{S} for both such families.

Joined elastic sectors

Consider now that the elastic sector is bordered by another elastic sector and that only the ray between them is stressed to yield. Call this ray $\theta = \theta^1$. Then one must have $N_\alpha^1 S_\beta^1 \dot{\sigma}_{\alpha\beta} > 0$ for some θ values in any range with $\theta < \theta^1$, and $N_\alpha^1 S_\beta^1 \dot{\sigma}_{\alpha\beta} < 0$ for some θ values in any range with $\theta > \theta^1$. Thus we conclude that $(N_\alpha^1 e_\alpha)(S_\beta^1 e_\beta)(B_\lambda e_\lambda)$ must change sign, from negative to positive, as θ increases through the value θ^1 . Here the B 's must be considered to be different in the two regions, and that means that a velocity discontinuity (implied by (22), at least near $r = 0$, for discontinuous B 's) will occur between them.

Drugan and Rice (1984) showed that a velocity discontinuity may move quasistatically through an ideal, plastically incompressible solid, satisfying an associated flow rule, provided that the (necessarily continuous) stress state at the discontinuity is consistent with zero extensional plastic strain rate in the plane of the discontinuity surface. Regarding the rays between sectors of the type considered here as candidate surfaces of velocity discontinuity, one sees that when a single family of slip plane traces, corresponding to N^1 and S^1 , is plastically active at a sector boundary, the boundary ray must have the direction of either N^1 or S^1 . Since these are orthogonal it is equivalent to require that either

$$N_\alpha^1 e_\alpha = 0 \quad \text{or} \quad S_\alpha^1 e_\alpha = 0 \quad (33)$$

for a velocity discontinuity to be allowed. Thus the ray direction e^1 , corresponding to θ^1 , must have the same line of action as either N^1 or S^1 . The velocity jump $[[v_\alpha]]$ must have the direction of N_α^1 or S_α^1 (whichever direction coincides with the discontinuity ray). Further, since $[[v_\alpha]]$ is proportional to $[[B_\alpha]]$ near $r = 0$ at a sector boundary, $[[B_\alpha]]$ is similarly restricted as to direction.

We thus see that the quantity $(N_\alpha^1 e_\alpha)(S_\beta^1 e_\beta)$ ($B_\lambda e_\lambda$), noted above to necessarily change sign as θ passes through θ^1 , does so by virtue of having one (only) of the first two factors vanish at θ^1 . Evidently, then, $B_\lambda e_\lambda$ must be nonzero and of the same sign on both sides of the discontinuity.

While $N_\alpha^1 S_\alpha^1 \dot{\sigma}_{\alpha\beta} = 0$ at $\theta = \theta^1$, $\dot{\sigma}_{\alpha\beta}$ is not zero in general at or near θ^1 (by (21) and (25), since $B_\lambda e_\lambda$ is nonzero near θ^1). Thus if we plot the stress combinations $\frac{1}{2}(\sigma_{11} - \sigma_{22})$ and σ_{12} as a function of θ , the resulting trajectory must touch the corresponding yield locus flat segment tangentially at $\theta = \theta^1$. This will happen as the flat is approached from both sides (look ahead to point B/C in Fig. 6(d)) since $B_\lambda e_\lambda \neq 0$ on both sides.

Restrictions on elastic sectors at $\theta = 0$ or π

It may be noted also that fields within elastic sectors must be severely restricted if these are to border either $\theta = 0$ or $\theta = \pi$. Since $e_2 \equiv \sin \theta = 0$ at those angles, σ_{11} would become logarithmically infinite as they are approached unless $B_1 = 0$. Further, the symmetry compatible with tensile loading requires that $B_2 = 0$ also for an elastic sector that includes $\theta = 0$.

Assembly of sectors for growing crack

Figures 6(b), (c) and (d) show the assembly of sectors for a growing crack. This assembly may be regarded as the analog for the crystals considered of what Slepyan (1974), Gao (1980), Gao and Hwang (1981) and Rice et al. (1980) have presented as the solution for the growing crack in an isotropic ideally plastic material, in solutions which are unobjectional for solids that are elastically as well as plastically incompressible, and of what Drugan et al. (1982) have presented for an elastically compressible ideally plastic Mises solid ($\nu \neq \frac{1}{2}$). When presented, those near tip stress fields were thought to be unique. Drugan and Chen (1987) have recently shown that they are not and that, instead, a family of qualitatively similar fields may exist in satisfaction of all equations of the asymptotic analysis. After constructing a particular solution here it will later be indicated how a family of similar solutions might be constructed,

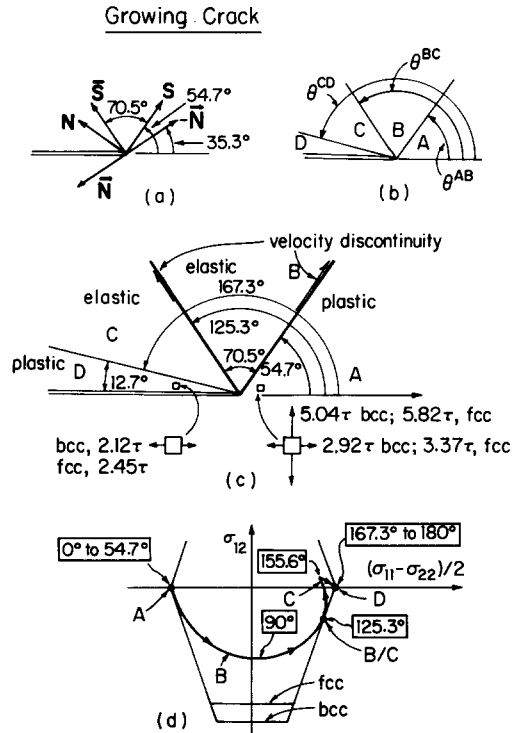


Fig. 6. Field at quasistatically growing crack in fcc or bcc crystal. (a) Vectors for two inclined families of slip planes traces in fcc crystal. (b) Definitions of angles at sector boundaries. (c) Sectors at crack tip, for fcc and bcc orientation considered, with slip velocity discontinuities along rays at $\theta^{AB} = 54.7^\circ$ and $\theta^{BC} = 125.3^\circ$. (d) Corresponding regions on yield locus and stress trajectory within elastic sectors B and C.

analogous to that identified by Drugan and Chen (1987).

Consider for definiteness the fcc geometry of Fig. 1 (the solution for bcc will differ only by a simple rescaling of the stress state due to the different β). The stress state directly ahead of the crack, on $\theta = 0$, cannot be below yield, for then $\theta = 0$ would lie in an elastically responding sector. As discussed earlier, such a sector would have $B_1 = B_2 = 0$, which converts it to a constant stress sector. Since no discontinuous changes in stress are now allowed, the stress could never reach yield and thus, to satisfy crack surface boundary conditions, the stress state would have to be of the form $\sigma_{11} = \text{constant}$, $\sigma_{21} = \sigma_{22} = 0$. This field is of no interest in the present context.

We therefore consider the stress directly ahead

of the crack to be at yield, which means that a constant stress sector exists ahead of the crack. Assuming that $\sigma_{22} > \sigma_{11}$ there, this state must correspond to the vertex marked *A* in Figure 6(d). Since such a stress state will be incompatible with crack surface boundary conditions when $\sigma_{22} \neq 0$, the stress must ultimately vary from that constant state. Such may happen only by transition to an elastic unloading sector. In terms of the labelling of vectors *N*, *S* and \bar{N} , \bar{S} in Fig. 6(a) associated with the two inclined fcc slip plane traces, the constant stress state in sector *A* satisfies

$$N_\alpha \sigma_{\alpha\lambda} S_\lambda = \beta\tau, \quad \bar{N}_\alpha \sigma_{\alpha\lambda} \bar{S}_\lambda = -\beta\tau, \quad (34)$$

and thus the stress rates at the border $\theta = \theta^{AB}$ of the elastic sector *B* (see Fig. 6(b)), in $\theta > 0$, must satisfy

$$N_\alpha \dot{\sigma}_{\alpha\lambda} S_\lambda \leq 0, \quad \bar{N}_\alpha \dot{\sigma}_{\alpha\lambda} \bar{S}_\lambda \geq 0 \quad (35)$$

which convert to

$$N_\alpha e_\alpha S_\beta e_\beta B_\lambda e_\lambda \geq 0, \quad \bar{N}_\alpha e_\alpha \bar{S}_\beta e_\beta B_\lambda e_\lambda \leq 0 \quad (36)$$

at e^{AB} , corresponding to θ^{AB} .

The elastic sector has a velocity singularity as $r \rightarrow 0$. To construct a specific solution, we assume that the velocity remains bounded within the plastic sector, ahead of the tip, as $r \rightarrow 0$. Thus there will be a velocity discontinuity $[[v_\alpha]]$ at θ^{AB} with $[[v_\alpha]]$ having the direction of B_α^B (the superscript refers to sector *B*) as $r \rightarrow 0$. To avoid a normal velocity discontinuity, B_α^B must be colinear with e_α^{AB} . Now, to be consistent with the flow rule at the vertex state of *A* the ray θ^{AB} of velocity discontinuity cannot lie outside the range generated by moving anti-clockwise from the ray $e = -\bar{N}$ to the ray $e = S$. The former with $B_\alpha e_\alpha > 0$ corresponds to (negative) shear relative to the \bar{N} , \bar{S} family of slip plane traces, and none on the other, and the latter with $B_\alpha e_\alpha > 0$ to (positive) shear relative to the *N*, *S* family, and none on the other; $B_\alpha e_\alpha > 0$ is required for any ray within the allowable range. However, if we use $B_\alpha e_\alpha > 0$ in (36), it is seen that θ^{AB} cannot lie outside the range generated by moving anti-clockwise from the ray $e = S$ to the ray $e = N$, and neither can it lie outside that generated by going anti-clockwise from $e = -\bar{N}$ to $e = \bar{S}$.

There is a unique value of e meeting those various requirements and it is $e^{AB} = S$. Thus the sector border lies along an active slip plane trace emanating from the crack tip (for the fcc material; that border will be perpendicular to the active slip plane traces for the bcc material). This coincidence means that the discontinuity involves shear relative to the *N*, *S* family of slip plane traces only. Also, $N_\alpha \dot{\sigma}_{\alpha\beta} S_\beta = 0$ at the beginning of the elastic unloading sector at θ^{AB} , so the stress trajectory in the $\frac{1}{2}(\sigma_{11} - \sigma_{22})$, σ_{12} plane begins with tangency to the segment of yield surface that is activated; see Fig. 6(d). The values of B_α^B are thus

$$B_\alpha^B = m S_\alpha \quad \text{where } m > 0 \quad (37)$$

and *m* remains to be determined.

It is not possible to choose *m* so that the stress trajectory in the elastic sector continues to $\theta = \pi$, meeting the crack surface boundary conditions, without violating the yield condition. This could be expected since the condition $B_1^B = 0$ is not met. Thus the stress trajectory must bump into the yield surface at some value of θ between θ^{AB} and π . This bump for the case examined lies along the flat segment of yield locus corresponding to active shear along the family of slip plane traces associated with \bar{N} , \bar{S} . The angle θ^{BC} at which the yield condition $\bar{N}_\alpha \sigma_{\alpha\lambda} \bar{S}_\lambda = \beta\tau$ for that system is attained depends on *m*. It turns out that the direction of the radial vector e^{BC} , corresponding to θ^{BC} (Fig. 6(b)), must be the direction \bar{S} . We will see why matters could not be otherwise soon but will continue here assuming that to be the case. Then, for that choice of θ^{BC} we meet the condition for one elastic sector to border on another, as discussed previously. To generate an admissible velocity discontinuity at the border θ^{BC} it is necessary that

$$B_\alpha^C = B_\alpha^B + \bar{m} \bar{S}_\alpha = m S_\alpha + \bar{m} \bar{S}_\alpha \quad \text{where } 0 < \bar{m}, \quad (38)$$

in region *C*, which is also an elastic sector. This equation assures that the (second) velocity discontinuity is consistent with shear in a positive sense relative to a slip plane trace of direction \bar{S} emanating from the crack tip.

The remaining strategy is to choose the extent of sector *C*, which ends at an angle θ^{CD} (Fig. 6(b))

to be determined, and the constant \bar{m} such that the stress trajectory in Fig. 6(d) passes through the vertex identified as *D* on the yield locus at θ^{CD} . If such an angle exists with $\theta^{BC} < \theta^{CD} < \pi$, and with $\bar{m} > 0$, and if the resulting stress trajectory does not pass outside the yield locus, then a solution has been obtained. The field is extended over the final sector, *D*, as a constant stress state which is at yield, corresponding to the vertex at *D*.

Thus, to determine *m* one requires that $\bar{N}_\alpha \sigma_{\alpha\lambda}^{BC} \bar{S}_\lambda - \bar{N}_\alpha \sigma_{\alpha\lambda}^{AB} \bar{S}_\lambda = 2\beta\tau$, giving

$$2\beta\tau = -m \int_{\theta^{AB}}^{\theta^{BC}} \left[\frac{S_\lambda e_\lambda \bar{S}_\alpha e_\alpha \bar{N}_\beta e_\beta}{e_2 c_{11}} \right] d\theta \quad (39)$$

where (28) is used with $B_\lambda^B = mS_\lambda$. The integrand is negative, because $\bar{N}_\beta e_\beta$ is, and thus this provides a solution for *m* with $m > 0$. Once *m* is determined, one uses (28) and the known values $\sigma_{12}^A = 0$, $(\sigma_{11}^A - \sigma_{22}^A) = -\beta\tau/S_1 S_2$ to compute the corresponding stresses at the *BC* interface:

$$\begin{aligned} \sigma_{12}^{BC} &= -m \int_{\theta^{AB}}^{\theta^{BC}} [e_1 S_\lambda e_\lambda / c_{11}] d\theta \\ \sigma_{11}^{BC} - \sigma_{22}^{BC} &= -\beta\tau/S_1 S_2 \\ &\quad + m \int_{\theta^{AB}}^{\theta^{BC}} \left[\frac{(e_2^2 - e_1^2) S_\lambda e_\lambda}{e_2 c_{11}} \right] d\theta. \end{aligned} \quad (40)$$

Next, we require that \bar{m} and θ^{CD} be chosen so that the stress trajectory hits the vertex at *D*, at which $\sigma_{12}^D = 0$ and $\sigma_{11}^D - \sigma_{22}^D = \beta\tau/S_1 S_2$. Using (28), with B_λ^C given by (38), this requires

$$\begin{aligned} 0 &= \sigma_{12}^{BC} - (mS_\lambda + \bar{m}\bar{S}_\lambda) \int_{\theta^{BC}}^{\theta^{CD}} \left[\frac{e_1 e_\lambda}{c_{11}} \right] d\theta, \\ \beta\tau/S_1 S_2 &= (\sigma_{11}^{BC} - \sigma_{22}^{BC}) \\ &\quad + (mS_\lambda + \bar{m}\bar{S}_\lambda) \\ &\quad \times \int_{\theta^{BC}}^{\theta^{CD}} \left[\frac{(e_2^2 - e_1^2) e_\lambda}{e_2 c_{11}} \right] d\theta. \end{aligned} \quad (41)$$

Because of the linear dependence on \bar{m} , one may solve the first of these for \bar{m} in terms of θ^{CD} , and then insert that result for \bar{m} into the second to obtain a single equation for θ^{CD} which can be solved numerically by standard root-finding procedures.

Finally, σ_{22} must be zero on the crack faces and

thus is zero in the constant stress sector *D*. Its value at any angle θ in the range $\theta^{AB} < \theta < \theta^{CD}$ corresponding to the two elastic sectors is thus given from (28) as

$$\sigma_{22} = \int_{\theta}^{\theta^{CD}} \left[\frac{e_2 B_\lambda e_\lambda}{c_{11}} \right] d\theta \quad (42)$$

where $B_\lambda = mS_\lambda + \bar{m}\bar{S}_\lambda$ for $\theta^{BC} < \theta < \theta^{CD}$ and $B_\lambda = mS_\lambda$ for $\theta^{AB} < \theta < \theta^{BC}$. The uniform value of σ_{22} in the constant stress plastic sector ahead of the crack is given by setting $\theta = \theta^{AB}$ in this equation.

Results

For the geometry considered, $\theta^{AB} = \arctan\sqrt{2} = 54.74^\circ$ and $\theta^{BC} = \pi - \theta^{AB} = 125.26^\circ$, corresponding to the two inclined families of {1 1 1} slip plane traces for the fcc case (and to the directions of normals to the families of {1 2 1} slip plane traces for the bcc case). For simplicity the elasticity is treated as isotropic so that $c_{11} = (1 - \nu)/2\mu$. One then obtains that

$$m = 2.560(1 - \nu)\beta\tau/\mu \quad (43)$$

and that $\sigma_{11}^{BC} = -0.426\beta\tau$, $\frac{1}{2}(\sigma_{11}^{BC} - \sigma_{22}^{BC}) = 0.910\beta\tau$. The extreme negative value of σ_{12} in sector *B* occurs at $\theta = 90^\circ$ and is $-0.910\beta\tau$, which falls well short of the flat segments cutting the σ_{12} axis in the yield loci of Figs. 1(c) and 2(c). The further results are

$$\bar{m} = 0.555(1 - \nu)\beta\tau/\mu, \quad (44)$$

which is only about 22% the strength of the first velocity discontinuity, and

$$\theta^{CD} = 167.30^\circ \quad (45)$$

so that the trailing plastic sector *D* has a 12.70° range. The resulting stress trajectory in the elastic sectors is indicated in Fig. 6(d); the cusp corresponds to the angle θ at which $B_\lambda^C e_\lambda = 0$. The maximum value of σ_{22} , which occurs in sector *A*, is

$$\sigma_{22}^A = 5.042\beta\tau. \quad (46)$$

It should be recalled that $\beta = 2/\sqrt{3} = 1.155$ and τ is the resolved shear strength for {1 1 1}⟨1 1̄ 0⟩ slip in the fcc case. Thus $\sigma_{22}^A = 5.82\tau$ in that case,

versus 7.35τ for the stationary crack. In the bcc case $\beta = 1$ and τ is the strength τ_{121} for $\{1\ 2\ 1\}\langle 1\ \bar{1}\ 1\rangle$ slip, at least when $\tau_{121} < (2/\sqrt{3})\tau_{101}$. Then, $\sigma_{22}^A = 5.04\tau$, compared to 6.69τ for the stationary crack. When the inequality is violated $\beta = 2/\sqrt{3}$ and τ is τ_{101} for $\{1\ 0\ 1\}\langle 1\ 1\ \bar{1}\rangle$ slip.

Again, it is emphasized that while the velocity discontinuities at $\theta = 54.74^\circ$ and 125.26° lie along slip plane traces for the fcc case, they occur at the same angles and thus lie perpendicular to the active slip plane traces in the bcc case and hence correspond then to a kink-like shear mode like in Fig. 5(b).

Remaining issues

First, why is the location chosen for θ^{BC} , along the slip plane trace of direction \bar{S} in Fig. 6(a), the only possibility? Suppose θ^{BC} is larger than that value. The elastic sector B can then only be trailed by a constant stress plastic sector, and that sector would have nonzero σ_{12} so that its stresses could not meet crack surface boundary conditions. Further, once into such a sector there would be no possibility of departing from it, into another elastic sector at large θ , because of the then inadmissible velocity discontinuity forced at the onset of an elastic unloading sector.

Suppose, then, that θ^{BC} is smaller than the value corresponding to the direction \bar{S} . Once again the sector B must be trailed by a constant stress plastic sector, and since the boundary angle θ^{BC} is then unfit for a velocity discontinuity, the velocity within the trailing plastic region must be continuous with that in elastic sector B . The latter velocity distribution is unbounded at $r=0$ and controlled by amplitude factors $B_\lambda^B = mS_\lambda$ with $m > 0$. Since the plastic region can only deform by single slip, relative to the \bar{N} , \bar{S} family, it is a straightforward matter to determine the velocity field in that region. The \bar{N} and \bar{S} directions are orthogonal characteristics for the velocity field, whose component along a given characteristic direction remains uniform along that characteristic line. One thereby computes the velocity field in the plastic sector but, when its resulting strain rates are computed, they are not of a sign consistent with positive plastic work by the given stresses. Thus this possi-

bility must be disregarded too, leaving the choice that θ^{BC} corresponds to the direction of \bar{S} as the only one possible.

Second, following concepts analogous to those of Drugan and Chen (1987), here is how a family of solutions might be generated: Suppose that the singular structure of the velocity field as in (22) holds not just in elastic sectors but in plastic sectors too. Thus in sector A one assumes that

$$\begin{aligned} v_1 &= \dot{a} [B^A \ln(R/r) + g_1(\theta)], \\ v_2 &= \dot{a} g_2(\theta). \end{aligned} \quad (47)$$

Here $B_2 = 0$ for reasons of symmetry and $B_1 = B^A = \text{constant}$. In this case the sector boundaries for B still occur at the angles θ^{AB} and θ^{BC} indicated in the solution just presented but now one must write

$$\begin{aligned} B_\lambda^B &= B^A \delta_{\lambda 1} + mS_\lambda, \\ B_\lambda^C &= B^A \delta_{\lambda 1} + mS_\lambda + \bar{m}\bar{S}_\lambda \end{aligned} \quad (48)$$

in sectors B and C , where $m > 0$ and $\bar{m} > 0$. The solution just presented corresponds to $B^A = 0$, but solutions for $B^A > 0$ will presumably lead to different values of m , \bar{m} , θ^{CD} and σ_{22}^A .

The plastic strain rate in sector A must admit the representation

$$\begin{aligned} &(\dot{a}\Lambda/r)(N_\alpha S_\beta + N_\beta S_\alpha) \\ &- (\dot{a}\bar{\Lambda}/r)(\bar{N}_\alpha \bar{S}_\beta + \bar{N}_\beta \bar{S}_\alpha) \end{aligned} \quad (49)$$

where $\Lambda \geq 0$ and $\bar{\Lambda} \geq 0$. By equating this to the strain rates $\partial v_\alpha/\partial x_\beta + \partial v_\beta/\partial x_\alpha$ computed from (47), and multiplying both sides with $e_\alpha e_\beta$ one finds

$$B^A e_1 = \Lambda (-N_\alpha e_\alpha)(S_\beta e_\beta) + \bar{\Lambda} (\bar{N}_\alpha e_\alpha)(\bar{S}_\beta e_\beta) \quad (50)$$

(other products, with $e_\alpha e'_\beta$ and $e'_\alpha e'_\beta$, involve the g'_λ and are not illuminating, except to convince that suitable g 's can be found so that Λ and $\bar{\Lambda}$ can be arbitrarily varying functions of θ within the constraint of (50)). On the line $\theta = 0$, $e_1 = 1$, Λ and $\bar{\Lambda}$ are equal by symmetry and their coefficients are both equal and positive. Thus

$$B^A = (\Lambda + \bar{\Lambda})(-N_1 S_1) = 2\Lambda S_1 S_2 \quad \text{on } \theta = 0. \quad (51)$$

Thus $B^A \geq 0$ is required. Now examine the ray $e = S$, corresponding to the sector boundary θ^{AB} . In that case the coefficient of Λ vanishes and one has, formally,

$$B^A S_1 = \bar{\Lambda} (\bar{N}_\alpha S_\alpha) (\bar{S}_\beta S_\beta) \quad \text{on } \theta = \theta^{AB}. \quad (52)$$

But the coefficient of $\bar{\Lambda}$ is negative in this expression whereas the left side of the equation is positive, and that is inconsistent with $\bar{\Lambda} \geq 0$. A way out of this dilemma is to assume that Λ becomes positive infinite as $\theta \rightarrow \theta^{AB}$ from below, particularly with Λ having the structure

$$\Lambda \sim (\text{positive constant}) / (-N_\alpha e_\alpha) \quad (53)$$

for θ near θ^{AB} .

This is analogous to a corresponding infinity of plastic work rate for the isotropic case (which occurs then as $\theta \rightarrow \frac{1}{4}\pi$). The analyses of Drugan et al. (1982) and the earlier works mentioned disregarded this possibility on the grounds that such fields involve an unbounded total plastic work per unit crack growth, and thus dealt with the case $B^A = 0$ only. However, Drugan and Chen (1987) recently pointed out for the isotropic case that such an objection is valid only if the sector boundary remains straight at nonzero r near the crack tip. In an ingenious analysis they show that curvature of the sector boundary at the crack tip, of an amount that increases with the size of their parameter analogous to B^A , removes the unbounded plastic work per unit crack growth, thus legitimizing a family of near tip fields where previously a single one was thought unique. While solutions with $B^A > 0$ have not been pursued in further detail here, it seems likely that they could be similarly rationalized by assuming curvature of the sector boundary which cuts into the crack tip at θ^{AB} .

Crack on the (1 0 1) plane

All the results presented here so far are for the case when the crack is on the (0 1 0) plane and is growing in the [1 0 1] direction, as in Figs. 1(a), (b) and 2(a), (b). Another interesting case is for the crack on the (1 0 1) plane with growth in the [0 1 0] direction. This corresponds to rotating the

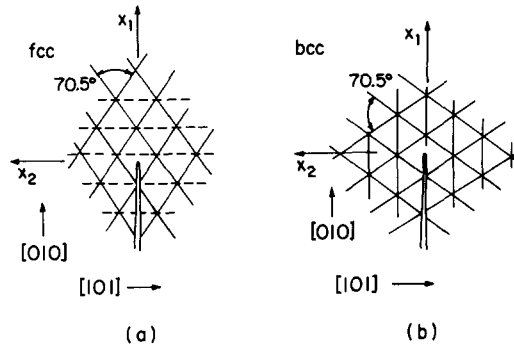


Fig. 7. Crack on (1 0 1) plane, with tip along [1 0 1] and [0 1 0] growth direction in (a) fcc and (b) bcc.

crack planes of Figs. 1(b) and 2(b) about the crack tips by 90° relative to the crystal, while the direction of the crack tip itself remains fixed (as [1 0 1]). The results are shown in Fig. 7.

Since this simply corresponds to a 90° rotation of all families of slip plane traces, relative to the orientations shown in Figs. 1(b) and 2(b), it corresponds to interchange of N for S and S for N on each family. The yield locus is unaltered by this operation, and thus the same yield loci as shown in Figs. 1(c) and 2(c) apply, respectively, for the cracks of Figs. 7(a) and (b). Thus the near tip solution for stress and deformation, relative to the x_1, x_2 axes shown, will be fully identical (within the small displacement gradient formulation, neglecting lattice rotation effects) to what has been presented here for cracks on (0 1 0) planes in the same type of crystal.

The physical difference is that a discontinuity which occurred along a slip plane trace for the (0 1 0) crack will instead occur along a normal to the corresponding slip plane traces for a (1 0 1) crack, and vice-versa. Thus, in terms of concentrated shear deformation on planes emanating from the tip, as discussed in connection with Figs. 3(a) and 6(c), regular shear zones, lying along a slip plane trace like in Fig. 5(a) for the (0 1 0) crack, become kink-like shear zones like in Fig. 5(b) for the (1 0 1) crack, and kink-like zones for the (0 1 0) crack become regular zones for the (1 0 1) crack.

Concluding discussion

Crack tip stress distributions and some constraints on near tip deformations have been derived within the small displacement gradient formulation for stationary and quasistatically growing plane-strain tensile cracks in ideally plastic single crystals. Face centered and body centered cubic solids are considered with (0 1 0) cracks growing along the [1 0 1] direction and with (1 0 1) cracks growing along [0 1 0].

For a stationary crack under rising load, the near tip stress state is uniform (independent of θ) within finite angular sectors at the crack tip, and the stress state jumps discontinuously at boundaries between sectors. The stress state in each sector corresponds to that of a vertex on the yield surface, at which two families of slip plane traces are simultaneously stressed to yield levels. The boundary between neighboring sectors, at which the stress state jumps from that of one vertex to that of an adjacent vertex, has an orientation coincident either with the slip plane traces or with their normals for that family of slip plane traces which is stressed to yield levels at both the adjacent vertices. (The stress state directly ahead of the tip, and on the crack faces, would not correspond to vertices in a crystal whose yield locus had no vertices on the $\frac{1}{2}(\sigma_{11} - \sigma_{22})$ axis.)

The stationary crack stress state requires a flow field in which concentrated plastic shear occurs along the sector boundaries, i.e., for which the boundaries are surfaces of slip displacement discontinuities. Such discontinuities are known to occur in the analogous anti-plane shear solutions (Rice and Nikolic, 1985) for stationary cracks in ideally plastic crystals.

For the quasistatically growing crack, neither the stresses nor the displacements can be discontinuous. This necessitates the presence of elastic unloading and reloading sectors at the crack tip, for which a full analysis is given here. The near tip field constructed for the growing crack is found to involve two rays of slip velocity discontinuity emanating from the crack tip. The first occurs at $\theta = 54.7^\circ$, just at the border with an elastic sector which unloads from the plastic stress state in front of the crack. That elastic sector reloads again and

stresses at plastic yield levels are attained at $\theta = 125.3^\circ$, where a second but weaker slip velocity discontinuity occurs and elastic unloading begins again. That second elastic sector ultimately reloads to attain yield level stresses in a trailing plastic sector which occupies a 12.7° range from the crack face. The two θ values cited coincide, necessarily, with either directions of slip plane traces or directions of their normals for families which are brought to yield levels by the local stress state.

The moving velocity discontinuities leave in their wake finite, suddenly accumulated plastic strains. Since the velocity jump becomes infinite in proportion to $\ln(1/r)$ near the tip, so also do the suddenly accumulated strains.

In addition to the inclusion of strain hardening in future studies of this type, two other issues seem to be of importance. First, a geometrically rigorous formulation which accounts for finite strain and, notably, for rotation of crystal directions relative to the material should reveal important new features. In part, these relate to the details of opening of the crack at its tip, as studied by Neumann (1974b) already in a kinematical manner that is focused on the particular type of fully plastic field indicated on Fig. 4b. The clarification of such opening (and reclosing) processes seems important to fundamental understanding of fatigue and other types of crack growth. An additional feature is that the invariance of the present solutions to interchange of directions (S) and normals (N) to slip plane traces will no longer hold. For example, a crack growing along [1 0 1] on a (0 1 0) plane in a fcc crystal is predicted to have velocity discontinuities that lie along the inclined slip plane traces of Fig. 1(b), involving deformation like in Fig. 5(a). A similarly loaded crack growing along [0 1 0] on a (1 0 1) plane in the same crystal is predicted to have an identical velocity field but now the discontinuities lie perpendicular to the activated family of slip plane traces, Fig. 7(a), and involves kinking-type shear as in Fig. 5(b). The latter causes the lattice within the shear zone to rotate relative to the material and thus affects the resolved shear component of the stress field in a manner not accounted for in the present formulation. This may involve geomet-

rical hardening or softening, depending on the direction of rotation, and may have a substantial effect on the resulting deformation fields.

Second, it may prove useful to examine the implications of the present, and future, continuum plasticity solutions for crystals with regard to the dislocation generation and motion necessary to produce the predicted deformation. A tacit assumption of the continuum theory is that sources which can emit dislocations are distributed profusely throughout the material so that conditions for plastic flow can be phrased solely in terms of achieving an adequate local stress level (e.g., represented by a yield surface like in Figs. 1(c) and 2(c)), without worry as to whether a defect structure is actually present at the stressed location to enable plastic response to that stress.

Such considerations were emphasized by Rice and Nikolic (1985) in analysis of elastic-plastic crack tip response of crystals in anti-plane shear. They noted that the plastic response predicted on the basis of continuum plasticity for some crack and crystal orientations could be effected by screw dislocations nucleated at the crack tip and swept out along slip planes, whereas response predicted for other orientations required the presence of abundant internal sources (see, for example, Fig. 10 of Rice and Nikolic, 1985, and associated discussion).

Analogous issues arise here. In the absence of profuse sources, the dislocations required to generate regular shear deformations along slip plane traces, as in Fig. 5(a), could be nucleated at the crack tip and swept out along those slip planes as indicated schematically in Fig. 5(c). By contrast, the dislocation motion necessary to accomplish the kinking-shear mode of plastic response, Fig. 5(b), would seem to require profuse internal sources from which dislocation loops could spread in a dipole mode along the active slip planes, which are then perpendicular to the zone of macroscopic shear concentration. This spreading is illustrated schematically in Fig. 5(d). Effectively, macroscopic shear is accomplished by the dislocations forming tilt walls. It may be remarked that Tetelman and Robertson (1963) observed cracks to grow on the (0 1 0) plane in a [1 0 1] direction

in bcc Fe-3% Si crystals which had been hydrogen charged. In this case the solutions presented here suggest that shear along the inclined discontinuities in Figs. 3 and 6 will be of the kinking type; the {1 2 1} type slip planes of Figs. 2(a), (b) are activated with the macroscopic shear zone lying perpendicular to those planes. Thus the dislocation activity to produce the flow is expected to be of dipole type, much as in Fig. 5(d), and this seems quite compatible with what Tetelman and Robertson (1963, Figs. 1, 2 and 5) observed in their etching studies to reveal dislocations.

One might speculate that the kinking shear mode of plastic relaxation, which seems to require extensive pre-existing sources, would be less effective than the regular shear mode in relaxing a crack in circumstances for which source activation is relatively inhibited. Such may be due to low temperature or rapid loading rate. Thus, while a crack on (1 0 1) in a bcc crystal is predicted here to have an identical stress field to a crack on (0 1 0), assuming both have the same [1 0 $\bar{1}$] crack tip direction, the latter orientation which relaxes primarily by kink-like shear may be more prone to cleavage when the temperature is low or the strain rate is high. The usual cleavage plane in a bcc solid is indeed (0 1 0); e.g., that was the observed plane in the Tetelman and Robertson work mentioned above and in studies on Fe-3% Si by Vehoff and Neumann (1979, 1980). Following this concept, it may be expected that if a fcc solid were to cleave, it might be more prone to do so on (1 0 1) than on (0 1 0) because, in that case, it is the former orientation which relaxes primarily by kink-like shear. Again, macroscopically, both orientations are predicted here to have identical stress states. In this connection it is interesting that recent reports of cleavage-like fracture facets in some fcc solids, including normally ductile copper (Sieradzki and Newman, 1985; Pugh, 1985; Wang, 1987), do apparently involve cracking on the (1 0 1) plane. However fcc Ir, which seems to readily cleave, does so on (0 1 0) planes (Hecker et al., 1978), as does also Al in a cleavage-like brittle cracking mode induced by exposure to liquid Bi (Lynch, 1985).

Acknowledgement

This study was initiated under support of the NSF Materials Research Laboratory (Grant NSF-DMR-83-16979) at Harvard and completed under support of the Office of Naval Research (Contract N00014-85-K-0045). I am grateful to Ruzica Nikolic for assistance with the numerical calculation of θ^{CD} from equations (40) and (41) and also for her suggestion that the fcc yield surface adopted in the earlier stages of this study required the cut-offs now shown along the σ_{12} axis in Fig. 1(c).

References

- Booker, J.R. and E.H. Davis (1972), "A general treatment of plastic anisotropy under conditions of plane strain", *J. Mech. Phys. Solids* 20, 239.
- Drugan, W.J. and X.-Y. Chen (1987), "Plane strain elastic-ideally plastic crack fields for mode I quasistatic growth at large scale yielding—I. A new family of analytical solutions", *J. Mech. Phys. Solids*, in press.
- Drugan, W.J. and J.R. Rice (1984), "Restrictions on quasistatically moving surfaces of strong discontinuity in elastic-plastic solids", in: G.J. Dvorak and R.T. Shield, *Mechanics of Material Behavior, Studies in Applied Mechanics* 6, Elsevier, Amsterdam, 59.
- Drugan, W.J., J.R. Rice and T.-L. Sham (1982), "Asymptotic analysis of growing plane strain tensile cracks in elastic-ideally plastic solids", *J. Mech. Phys. Solids* 30, 447; erratum in *Vol. 31*, 391.
- Gao, Y.-C. (1980), "Elastic-plastic field at the tip of a crack growing steadily in perfectly plastic medium" (in Chinese), *Acta Mechanica Sinica* 1, 48.
- Gao, Y.-C. and K.-C. Hwang (1981), "Elastic-plastic fields in steady crack growth", in: S. Nemat-Nasser, ed., *Three-Dimensional Constitutive Relations and Ductile Fracture*, North-Holland, Amsterdam, 417.
- Garrett, G.G. and J.F. Knott (1975), "Crystallographic fatigue crack growth in aluminum alloys", *Acta Metallurgica* 23, 841.
- Hecker, S.S., D.L. Rohr and D.F. Stein (1978), "Brittle fracture in iridium", *Metallurgical Trans.* 9A, 481.
- Hill, R. (1950), *The Mathematical Theory of Plasticity*, Clarendon Press, Oxford.
- Hirth, J.P. and J. Lothe (1968), *Theory of Dislocations*, McGraw-Hill, New York.
- Lynch, S.P. (1983), "Environmentally assisted cracking—fractographic and mechanistic aspects, in: R. Latanision and T.E. Fischer, eds., *Advances in the Mechanics and Physics of Surfaces, Vol. 2*, Harwood Academic Publishers, New York, 265.
- Lynch, S.P. (1985), "'Cleavage' of aluminium single crystals in liquid metal environments", *Materials Science and Engineering* 72, L33.
- Neumann, P. (1974a), "New experiments concerning the slip processes at propagating fatigue cracks—I", *Acta Metallurgica* 22, 1155.
- Neumann, P. (1974b), "The geometry of slip processes at a propagating fatigue crack—II", *Acta Metallurgica* 22, 1167.
- Neumann, P., H. Fuhlrott and H. Vehoff (1979), "Experiments concerning brittle, ductile and environmentally controlled fatigue crack growth", in: J.T. Fong, ed., *Fatigue Mechanisms*, ASTM Spec. Techn. Publ. 675, p. 371.
- Pan, J. (1986), "Plane-strain crack-tip stress field for anisotropic perfectly-plastic materials", *J. Mech. Phys. Solids* 34, 617.
- Pugh, E.N. (1985), "Progress towards understanding the stress corrosion problem", *Corrosion-NACE* 41, 517.
- Rice, J.R. (1967), "Mechanics of crack tip deformation and extension by fatigue", in: *Fatigue Crack Propagation*, ASTM Spec. Techn. Publ. 415, 247.
- Rice, J.R. (1973), "Plane strain slip line theory for anisotropic rigid-plastic materials", *J. Mech. Phys. Solids* 21, 63.
- Rice, J.R. (1982), "Elastic-plastic crack growth", in: H.G. Hopkins and M.J. Sewell, eds., *Mechanics of Solids*, Pergamon Press, Oxford, 539.
- Rice, J.R. (1984), "On the theory of perfectly plastic anti-plane straining", *Mechanics of Materials* 3, 55.
- Rice, J.R., W.J. Drugan and T.-L. Sham (1980), "Elastic-plastic analysis of growing cracks", in: *Fracture Mechanics*, ASTM Spec. Techn. Publ. 700, 189.
- Rice, J.R. and R. Nikolic (1985), "Anti-plane shear cracks in ideally plastic crystals", *J. Mech. Phys. Solids* 33, 595.
- Rieux, P., J. Driver and J. Rieu (1979), "Fatigue crack propagation in austenitic and ferritic stainless steel single crystals", *Acta Metallurgica* 27, 145.
- Sieradzki, K. and R.C. Newman (1985), "Brittle behaviour of ductile metals during stress corrosion cracking", *Philosophical Magazine A* 51, 95.
- Sieradzki, K., R.L. Sabatini and R.C. Newman (1984), "Stress corrosion cracking of copper single crystals", *Metallurgical Trans. A* 15A, 1941.
- Slepyan, L.I. (1974), "Growing crack during plane deformation of an elastic-plastic body" (in Russian), *Izv. Akad. Nauk SSSR, Mekh. Tela* 9, 57.
- Tetelman, A.S. and T.L. Johnston (1965), "Plastically induced crack growth in iron-3% silicon monocrystals", *Philosophical Magazine* 11, 389.
- Tetelman, A.S. and W.D. Robertson (1963), "Direct observation and analysis of crack propagation in iron-3% silicon single crystals", *Acta Metallurgica* 11, 415.
- Vehoff, H. and P. Neumann (1979), "In-situ SEM experiments concerning the mechanism of ductile crack growth", *Acta Metallurgica* 27, 915.
- Vehoff, H. and P. Neumann (1980), "Crack propagation and cleavage initiation in Fe-2.6% Si single crystals under controlled plastic crack tip opening rate in various gaseous environments", *Acta Metallurgica* 28, 265.

Vitek, V. (1974), "Theory of the core structures of dislocations in body-centered-cubic metals", *Crystal Lattice Defects* 5, 1.

Vitek, V. (1985), "Effect of dislocation core structure on the plastic properties of metallic materials", in: M.H. Loretto, ed., *Dislocations and Properties of Real Materials*, The Institute of Metals, London, 30.

Wang, J.-S. (1987), "A new type of brittle fracture in a fcc metal bicrystal with intergranular segregation", *J. Materials Research*, in press.